

TRAJECTORY PREDICTION UNCERTAINTY MODELING FOR CONTINUOUS DESCENT APPROACHES

Gabriele Enea*, Robert Vivona*, David Karr*, Karen Cate**
***Engility Corporation, **NASA Ames Research Center**

Keywords: *continuous descent approach, trajectory prediction, uncertainty estimation,*

Abstract

One proposed approach to enabling Trajectory Based Operations, and Continuous Descent Approaches in congested airspace, is to use decision support technology with real-time trajectory prediction. A method for defining and quantifying models of real-time uncertainty estimation for use with such technology has been developed previously. A demonstration of this methodology for adding real-time estimation of altitude error to trajectory predictions in the Center/TRACON Automation System is provided. The methodology uses analysis of actual and predicted CDA trajectories obtained from Air Route Traffic Control Center operational data and from CTAS's trajectory synthesis process, respectively. Altitude error was aggregated over the flight sample through the application of statistical analysis at discrete altitude increments along the predicted descent trajectory. The evolution of altitude error mean and standard deviation was modeled in segments, each represented by an equation that best fit the aggregated data. Three segments describe the evolution of the standard deviation and four the evolution of the mean error. To illustrate the method an initial demonstration was performed with a limited data set. Given a larger set of data the final model could be generally applicable in generating an uncertainty model to support decision support technology in the performance of new arrival procedures such as CDA in congested airspace.

1 Introduction

Current arrival operations typically require aircraft to level off at a number of altitudes

during their approach to the destination airport. Although these procedures are easily managed by Air-Traffic Control (ATC), they result in higher-than-optimal fuel consumption and larger-than-necessary environmental impact. The Continuous Descent Approach procedure from en route airspace through the terminal area allows near-idle engine power operations during descent to the runway, increasing overall fuel efficiency and reducing noise and emissions. Safe and efficient CDA operations is one of the objectives for both the Next Generation Air Transportation System (NextGen) [1], envisioned by the Federal Aviation Agency (FAA), and for the Single European Sky Air Traffic Management Research (SESAR) [2] concept proposed by EUROCONTROL.

Although CDA operations are environmentally friendly and save fuel, they are more challenging than current operations for air traffic controllers because of the challenge in predicting relative aircraft spacing between aircraft performing near-idle descents, not to mention any crossing traffic. As a result it is unlikely that CDA operations will be supported in congested airspace without the utilization of controller-based Decision Support Tool (DST) technology. The En Route Descent Advisor (EDA) [3], a component of the Center/TRACON Automation System (CTAS), provides controllers with speed, altitude and path stretching advisories that have the potential to enable CDA operations to be performed in congested airspace under time-based metering [4]. Advisories are evaluated by conflict detection (CD) and resolution algorithms applied to modify the trajectories to ensure that they maintain sufficient aircraft spacing.

Trajectory prediction accuracy is key in that it drives the overall performance of the controller advisories. EDA uses a Flight Management System (FMS)-quality trajectory predictor (TP). The accuracy of the TP's nominal predicted trajectories has been evaluated during multiple field tests [5-7]. The results demonstrated the capability of the TP and highlighted the fact that some level of trajectory prediction uncertainty is intrinsic to the trajectory prediction process. Predicted trajectories are based on models of aircraft performance, forecasts of meteorological conditions, estimates of aircraft weight, clearances issued by controllers, and inferred pilot intent. All these models can include inaccuracies and approximations that, even if limited, cannot be completely eliminated or neglected.

The CTAS CD algorithms include a probabilistic uncertainty model [8],[9] for predictions of trajectories, including trajectories suitable for CDA operations. An appropriately quantified set of parameters, applied to this model of uncertainty in real time, could help EDA provide effective support for CDA operations in congested airspace.

A methodology to quantify the parameters of real-time uncertainty models was previously created by extending and applying prediction accuracy analysis techniques to uncertainty estimation modeling [10]. The objective of the research documented in this paper was to demonstrate how this methodology can be used to quantify the CTAS probabilistic uncertainty model for CDA operations and to validate the assumptions of the model for that purpose. This demonstration used a small, existing data set collected from other research efforts on CDA operations.

The following sections of this paper first summarize the CTAS probabilistic uncertainty model and the origins and nature of the data set used in the demonstration of uncertainty estimation. The quantification methodology is then applied to a small data set to estimate some parameters of the vertical dimension of uncertainty (altitude error) in CTAS trajectory predictions. This is followed by discussions of the validation of the model's assumptions and of the conclusions of the research effort.

2 CTAS Analytic Probabilistic Approach

The analytic probabilistic approach used in CTAS for real-time uncertainty estimation was developed by Paielli and Erzberger [8,9,11]. It models trajectory prediction error at any given time as a Gaussian distribution of possible actual positions of the aircraft around the predicted position at that time. Based on that model, the CTAS conflict detection algorithm computes an analytical solution for the probability that a conflict between the predicted trajectories of the two aircraft will actually occur. The CTAS probabilistic uncertainty model assumes the prediction error for each aircraft can be parameterized independently in the along-path, cross-track, and vertical dimensions; in three dimensions, the distribution can be said to have an ellipsoidal shape.

Another assumption of the model is that, in the vicinity of a conflict, the standard deviation¹ of the prediction error distributions' is approximately constant for the cross-track and altitude errors and linearly increasing for the along-track error. Although the original probabilistic uncertainty model starts from these preliminary assumptions they are not required by the conflict detection algorithm [9]. This paper focuses only on quantifying the uncertainty model in the vertical dimension. Therefore the basic assumptions that need to be validated during the quantification process are:

- The altitude error is approximately normally distributed
- The mean altitude error is small
- The standard deviation of the altitude error is nearly a linear function of time

3 CDA Data

Continuous Descent Approaches by definition require aircraft to descend to the destination (TRACON arrival meter fix or runway), without significant intermediate altitude level-offs, where possible. In some CDA definitions the maximum level flight phase allowed is 2.5

¹ Although in the references the model refers to the root mean square error, because the analysis assumes zero mean error, the root mean square error and the standard deviation are the same.

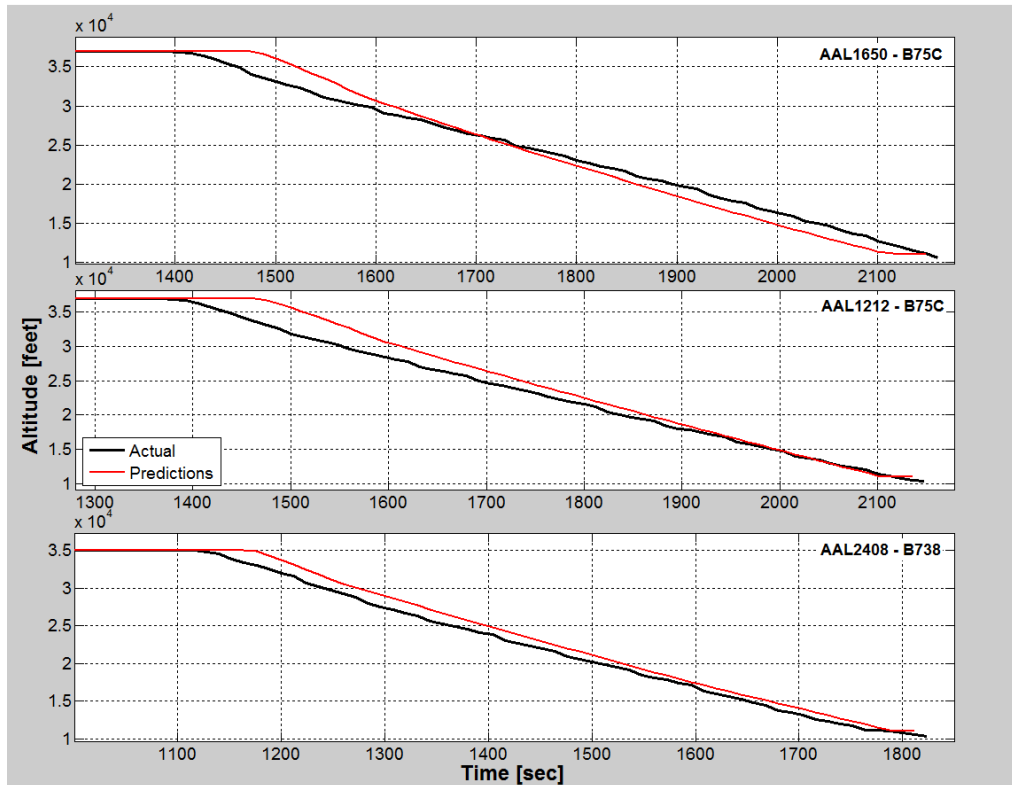


Figure 1 CDA vertical profiles, Dallas field test

nautical miles [12]. The quantification of the CTAS uncertainty model used data from three different NASA and FAA CDA field tests:

- Oceanic Tailored Arrivals (OTA) into San Francisco Airport performed by NASA Ames and the FAA (August 2006 and January 2007) [4]; ten flights, all Boeing 777
- CDAs into Dallas by NASA Ames North Texas (NTX) Facility (February 2008) [13]; three flights, two B757 and one B737
- CDAs into Miami Airport by the FAA (May 2008) [14]; six flights, three B777 and three B747

Although the CDA operations were performed at different airports and collected during different tests, the trajectories analyzed had similar cruise and final altitudes. The cruise altitudes were between 35,000 and 40,000 feet; the final altitudes were 16,000 feet for the Miami data and 11,000 feet for all other flights. The final altitude of each trajectory analyzed was at the meter fix on the TRACON boundary.

The data exchanged between ground and air during the three flight tests was also comparable. In the OTA field trial, atmospheric

characteristics, speed and clearance information were exchanged in real time. In the other two trials, the procedures were developed *a priori*; only a “descend via” clearance was issued by the controllers. In all three trials, each aircraft’s FMS calculated the Top of Descent (TOD) location without regard to the speed and altitude restrictions shared between ground and air. These characteristics suggest that the three data sets can be combined into a single sample representing a common procedure, which is characterized by a common level of TP uncertainty.

4 Preliminary Visualization

To visualize the variation in TP prediction uncertainty during a CDA, actual and predicted trajectories were plotted versus time for all flights. Visualizing the difference between actual and predicted trajectories provides insight into the evolution of prediction error and helps to identify the analyses required to quantify the uncertainty model. The CTAS probabilistic uncertainty model assumes an evolution of prediction error with time; therefore visualizing actual (observed) and predicted trajectories on

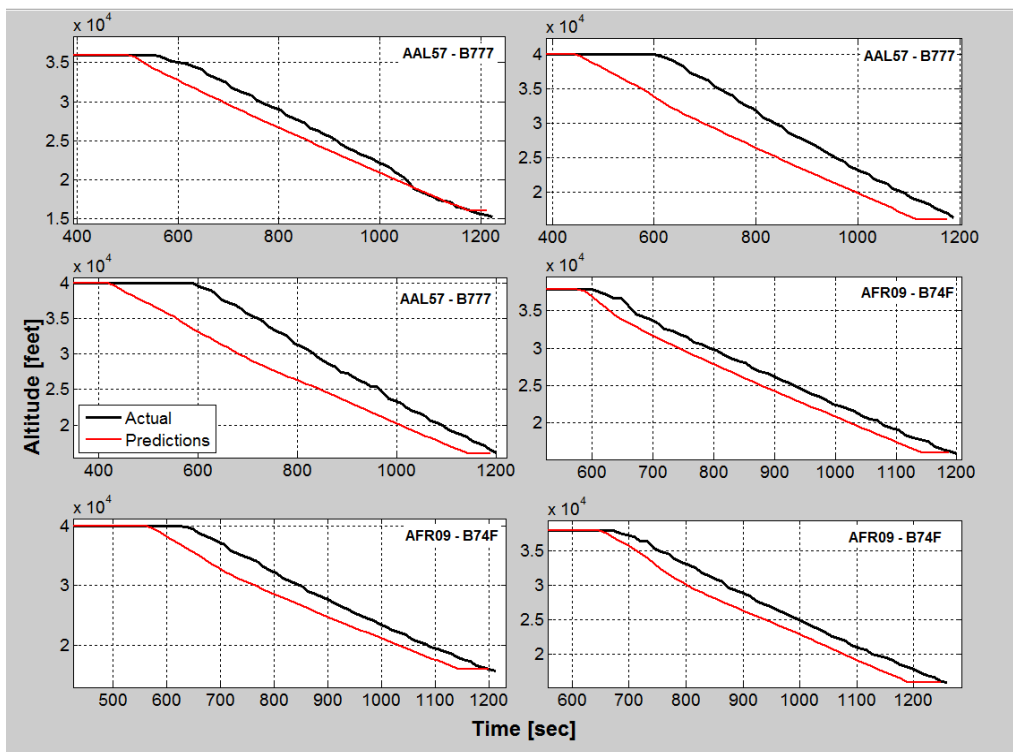


Figure 2: CDA vertical profiles, Miami field test

the same time scale (i.e., temporal correlation² [15]) was a logical starting point. This type of plot is useful to visually identify where the TP is more or less accurate and to identify where along the predicted trajectory the variation in prediction error changes behavior.

From Figure 1 it is observed that the three flights analyzed in the Dallas data descended earlier than the CTAS predicted TOD time. As a consequence, there were large negative altitude errors (actual altitude below predicted altitude) near the predicted TOD time. During the descent, the actual flight paths were shallower than the predicted paths, gradually decreasing the error towards the meter fix in two cases and actually reversing the error sign (actual altitude above predicted altitude) in the third. This same general behavior was also observed in the field tests performed by NASA Ames between 1992 and 1995 [5-7]; in those tests the FMS-equipped aircraft (some B737, B757, and A320) had a negative altitude error at predicted TOD as observed in the Dallas flights.

² The actual and predicted trajectories were temporally correlated at the first state predicted by CTAS which represents the x axis' zero in Figure 1 and Figure 2.

The opposite behavior can be observed for the CDAs into Miami (Figure 2), where the aircraft all descend after the predicted TOD time. This substantial difference in the error at predicted TOD could be caused by the different aircraft performance models in the CTAS TP. The B777 in two different flight tests (OTA and Miami) has the same behavior, being late at the predicted TOD. This significant difference in prediction error behavior could indicate the need for a separate uncertainty model for the B777 or possibly an adjustment to the CTAS TP for this aircraft type. The analysis described in this paper, the first application of the methodology, assumes the same uncertainty model for each aircraft type in the sample, including the B777. Grouping all the flights in one sample was the most rational choice having only a limited number of flights to analyze. The identification of both general and specific flight prediction error behaviors was one of the objectives of this preliminary visualization approach. An additional benefit of this step was the identification of this unique (possibly erroneous) behavior of the B777 predicted trajectories.

From the preliminary visualization it is clear that significant altitude errors occurred at the predicted TOD for almost all of the flights; previous studies indicated this same behavior [4,7]. To compare the prediction errors across the flight sample, a spatial correlation approach was employed. In general, a correlation approach defines which actual state (from the actual trajectory) is correlated with which predicted state during a prediction accuracy analysis [10]. Different types of correlation approaches are useful for different analysis purposes. For the purpose of this preliminary analysis, the observed event at a point was paired with the nearest point on the predicted trajectory, measured according to the lateral distance between the points. These two points were then considered to occur at the same *along-path distance*, defined as the distance along the predicted path from some predetermined reference point to the predicted point.³ An additional complexity existed because the predicted path distance from TOD to meter fix varied greatly among the flights in the data set. To deal with this issue, the flights were first spatially correlated relative to the predicted TOD, and then to the meter fix, and the altitude errors for each of these correlations were plotted as a function of the along-path distance relative to the correlated point as shown in Figure 3. In these plots the independent variable is:

$$s = \text{distance (nmi) along the predicted path, relative to the reference point}$$

The reference point identified with the zero in the abscissa (along path distance) represents, respectively, the predicted TOD and meter fix locations in the upper and lower plots of Figure 3. For locations along the predicted path before the reference point, s is negative. When the meter fix is the reference point, s is negative for all points plotted on the graph. The predicted and observed altitudes are then defined as functions of along-path distance:

$$\begin{aligned} h_{pred}(s) &= \text{predicted altitude (feet) as a function of along-path distance } s \\ h_{obs}(s) &= \text{observed altitude (feet) as a function of along-path distance } s \end{aligned}$$

The dependent variable in Figure 3 then is the altitude error, ε_h , defined as:

$$\varepsilon_h(s) = h_{obs}(s) - h_{pred}(s)$$

With this approach the common error trends around predicted TOD and meter fix were visible independent of the varying cruise and meter fix altitudes. From the plots in Figure 3 it is clear that the different data sets presented different evolutions of the altitude error over the predicted CDA trajectory.

To quantify the uncertainty model in the vertical dimension it was necessary to calculate the altitude error's standard deviation evolution over the CDA trajectory. The standard deviation represents the scatter of the altitude error, but not its sign; in fact the sign of the error was not relevant to identify error growth rate segments. From Figure 3, three different segments of the error variation rate were identified, i.e. an initial steep increase after the TOD, caused by the aircraft being late or early at TOD. A following decrease with a moderate slope, associated with the descent phase with no noticeable difference between the Mach and CAS segments. And a final steep decrease rate, related to the level-off deceleration segment predicted by CTAS between BOD and the meter fix. The length of these three segments needed to be quantified by aggregating the standard deviation of the error across all trajectories. The CTAS model was quantified, and the preliminary assumptions were then investigated as described in Section 6.

³ See reference [10] for additional details of spatial correlation.

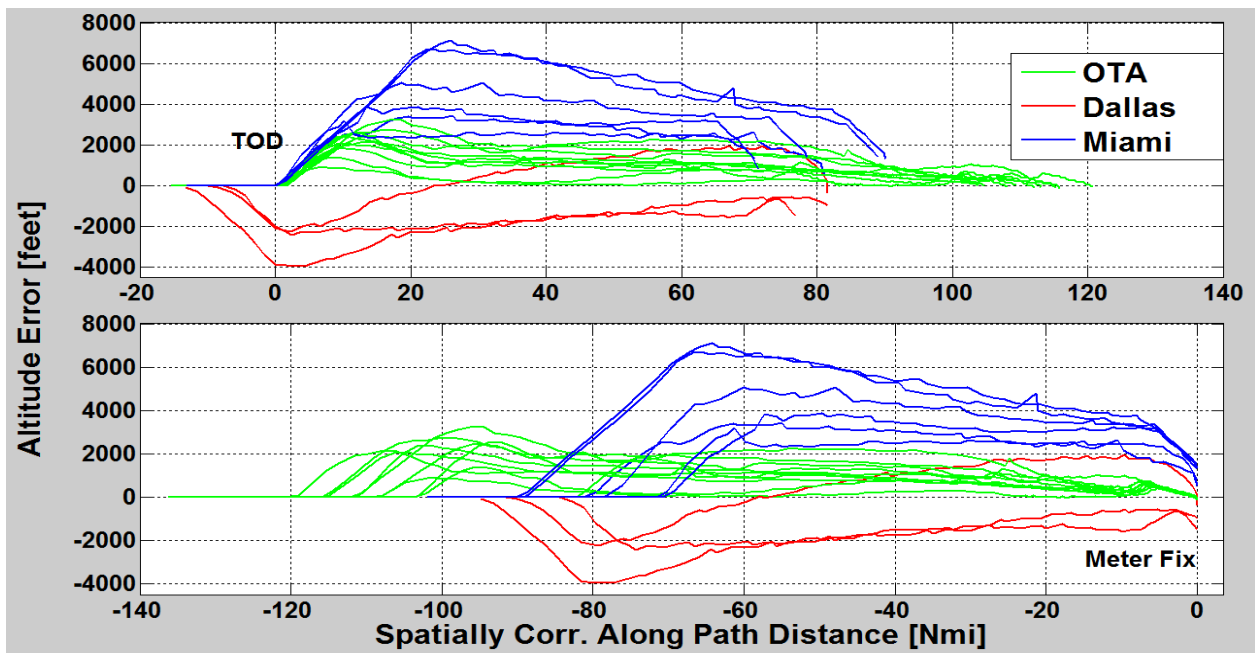


Figure 3: Altitude error spatially correlated at predicted TOD and meter fix

5 Assembling the Data for Analysis

The descent length across the flights in the sample was not homogenous; the altitude difference between the TOD and the meter fix in fact ranged from 20,000 to 28,000 feet, as shown in Figure 4.

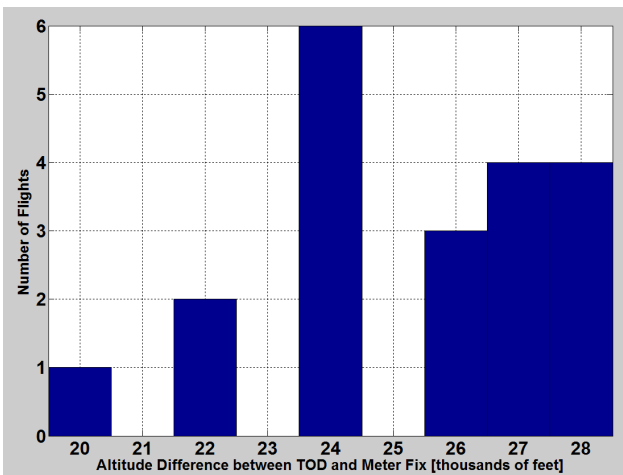


Figure 4 Distribution of the altitude difference between TOD and meter fix over the sample of flights

Ideally, analysis of the data would result in a model of uncertainty that would apply to descents with a wide variety of altitudes at TOD and meter fix. A sufficiently large set of trajectories with sufficient variation in these altitudes is desirable to support that analysis. In

the data available for the effort described here, however, almost all the flights had altitude differences in a relatively narrow range (24,000 to 28,000 feet), and each trajectory’s altitude difference depended largely on which field test produced the trajectory, suggesting that this variable would be correlated with other confounding variables.

For the purpose of demonstrating an analysis, therefore, the impact of the altitude difference was not investigated; instead, the data were artificially mapped to predicted trajectories that all descended from 38,000 feet at TOD to 11,000 feet at the meter fix, a difference of 27,000 feet (where the majority of the actual data were clustered).

In this specific treatment of the data, the top 10,000 feet of each predicted trajectory (from the TOD to a point predicted 10,000 feet below TOD) were mapped to the altitude range from 28,000 to 38,000 feet. The bottom 10,000 feet (from a point predicted 10,000 feet above the meter fix, down to the meter fix) were mapped to the altitude range from 11,000 feet to 21,000 feet. For each trajectory whose altitude difference was at least 24,000 feet, the central 4,000 feet of the predicted trajectory were mapped to the center of the new altitude range, 22,500 to 26,500 feet. Visual inspection of the middle 4,000 or more feet of each flight’s

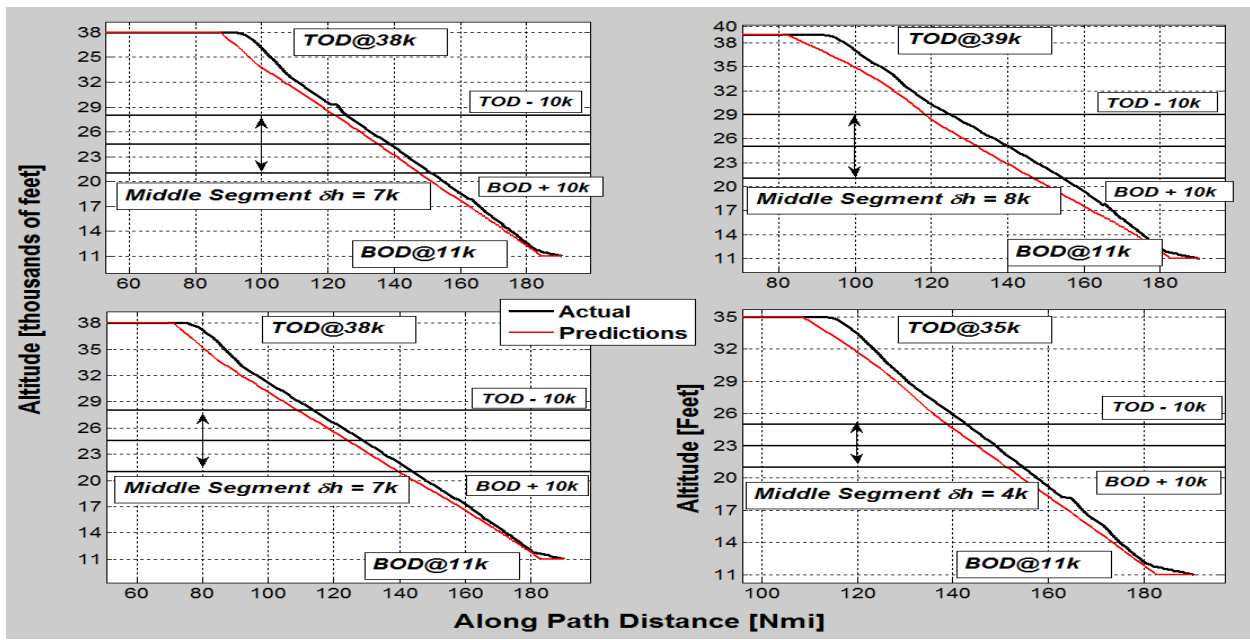


Figure 5: Flights with different middle segment

trajectories, both predicted and actual altitudes plotted against along-path distance, was performed to confirm that this altitude range captured the middle segment’s error behavior⁴ (Figure 5).

If there had been flights with descent length of less than 20,000 feet they would have contributed only to the top and bottom part of the model. The total descent length would have been divided in two; half of the data points would have been mapped to the segment below TOD and half to the segment below BOD.

6 Model Parameter Quantification

After grossly identifying the segments of the uncertainty model (section 4), the next step of the analysis was to quantify the evolution of the mean and standard deviation of the altitude error along the descent trajectory for each segment. Therefore, an approach was needed to aggregate each flight’s altitude error along its predicted trajectory over the complete sample of flights to calculate the model’s required error statistics.

For the portion of each predicted trajectory between the TOD and the BOD, a hybrid spatial-altitude correlation was used. For this

correlation method, predicted altitude was used as an independent variable:

$$h_{pred} = \text{predicted altitude (feet)}$$

Two dependent variables were defined as functions of the predicted altitude:

$$s(h_{pred}) = \text{Along-path distance (nmiles) at which the aircraft was predicted to reach the altitude } h_{pred}$$

$$h_{obs}(s) = \text{observed altitude (feet) as a function of along-path distance } s$$

The altitude error ϵ_h , was then calculated as:

$$\epsilon_h(h_{pred}) = h_{obs}(s(h_{pred})) - h_{pred}$$

This technique uses spatial correlation to measure any single altitude error along a predicted trajectory, but because it selects the events (i.e., along path locations at which to calculate the altitude error) by predicted altitude, it allows aggregating the errors from multiple flights at the same predicted altitudes.

The spatially correlated altitude error of each flight was calculated at defined predicted

⁴ This visual inspection assured that the data points left out (at 21,500, 22,000, 27,000, or 27,500 feet) didn’t present any anomalous altitude error behavior.

altitude steps in 500 ft increments within the available data.

One more complication was that the CTAS predicted trajectories included a bottom of descent (BOD) location, where the aircraft leveled off briefly to decelerate to a speed constraint at the meter fix. This level-off represents a slight discontinuity in CDA trajectory; it also prevents the use of altitude as an independent variable, since the entire segment is at one altitude. To cover the error evolutions between the BOD and the meter fix, the altitude error statistics were therefore calculated at three additional along-path distances: BOD, meter fix, and the point half-way between them. In order to analyze prediction error along this segment, we let:

$$s_{BOD} = \text{along path distance at the BOD}$$

$$s_{MF} = \text{along path distance at the meter fix}$$

Then the altitude error, ε_h , along this segment is defined by:

$$\varepsilon_h(s) = h_{obs}(s) - h_{pred}(s)$$

$$\text{for } s \in \{s_{BOD}, (s_{BOD} + s_{MF})/2, s_{MF}\}.$$

In order to aggregate these errors over multiple trajectories, we define the along-path distance as a linear function of a dimensionless variable, λ , such that

$$s(1) = s_{BOD}$$

$$s(0.5) = (s_{BOD} + s_{MF})/2$$

$$s(0) = s_{MF}$$

In this way we are able to plot all predicted level-off segments over a common range of the variable λ from 1 to 0.

From this data, the altitude error mean and standard deviation over the entire flight data set were calculated at each of these predicted altitudes and distances. For each flight, the altitude error were calculated at TOD (38,000

feet), at twenty consecutive points below the TOD altitude (down to 28,000 feet predicted altitude), nine points in the range from 26,500 down to 22,500 feet predicted altitude, twenty consecutive points above the BOD altitude (predicted altitudes 21,000 feet and below), and three between the BOD and the meter fix, for a total of fifty-three data points.

7 Model Representation

With the approach described in section 6 a sequence of altitude and spatial (between the TOD and meter fix) events along the entire CDA trajectory were defined. The altitude error mean and standard deviation across the flights were then calculated over each of these adapted data points. This aggregated data, except for the data for the level-off segment, were plotted against their predicted altitudes, as shown in Figure 6.

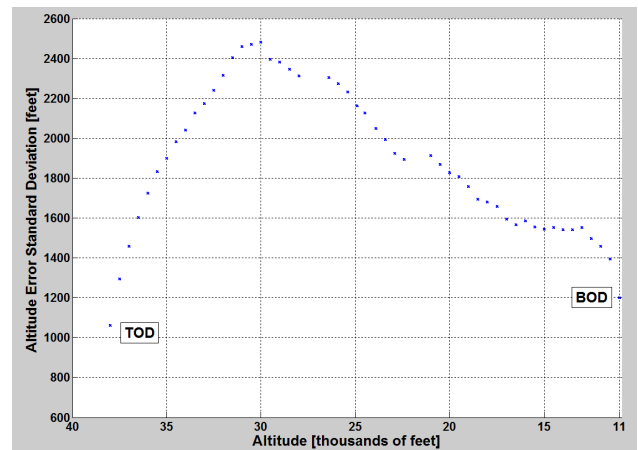


Figure 6: Altitude error standard deviation evolution

The data for the level-off segment were plotted against the dimensionless variable λ over the range 1 to 0, as shown in Figure 7.

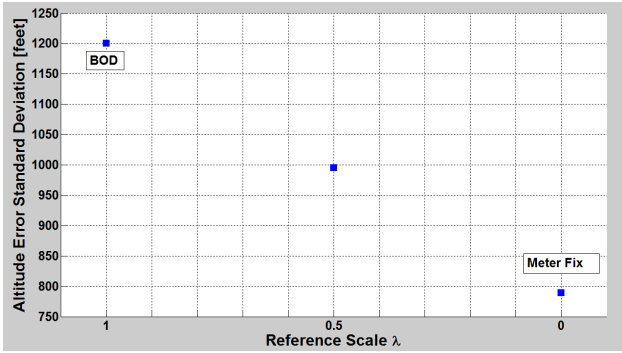


Figure 7: Altitude error standard deviation between BOD and the meter fix

8 Defining the Transitions between Model Segments

The analytic probabilistic approach in CTAS requires the quantification of the evolution (growth or decay rate) of the error standard deviation. To calculate these rates, the altitude error standard deviation at each altitude and spatial event was first plotted versus decreasing altitude from the predicted TOD for a reference altitude length of 27,000 feet to the predicted BOD (Figure 6). This altitude length, as mentioned before, was arbitrarily chosen to adapt the analysis to the data set; most of the altitude differences (TOD to meter fix) were in fact clustered around 27,000 feet (Figure 4).

From Figure 6 it is possible to see how the altitude error standard deviation rapidly grows after the predicted TOD to almost 2,500 feet in less than 10,000 feet of descent; this result is significant, because it is almost two and a half

times the minimum vertical separation. The standard deviation value then begins to decay slowly to the predicted BOD and then with a very steep rate to the meter fix as shown in Figure 7. From these plots it was possible to quantify, with an acceptable level of confidence, the three different segment rates grossly identified in the preliminary steps of the analysis (Section 4).

To complete the definition of the uncertainty model, the best mathematical representation for the three trends in standard deviation needed to be quantified. This was done by fitting a curve to this data using an exhaustive search algorithm implemented in MATLAB®. The algorithm determined, for all the possible combinations of initial and final data points in Figure 6, the value of the correlation coefficient between the actual standard deviation data and the regressed model. The search was based only on linear and quadratic regression curves. The correlation coefficient was defined as the Pearson's product moment correlation coefficient between STD (the standard deviation values) and REG (the data point of the regression analysis curve):

$$r = \frac{\sum_{i=1}^n (STD_i - \overline{STD})(REG_i - \overline{REG})}{\sqrt{[\sum_{i=1}^n (STD_i - \overline{STD})^2 \sum_{i=1}^n (REG_i - \overline{REG})^2]}}$$

where \overline{STD} and \overline{REG} are the sample means of the observed (standard deviation values) and

Segment	Altitude Range	STD Initial Value (ft)	STD Final Value (ft)	Evolution Equation (x = altitude in feet)*	Grow th/D eacy	Correlation coefficient with observed data
1	TOD→TOD-8k	1147	2477	$y = -1.63 \times 10^{-5}x^2 + 0.94x - 1147$	G	0.996
2	TOD-8k→BOD	2481	1366	$y = 8.17 \times 10^{-7}x^2 + 0.03x + 990$	D	0.987
3	BOD→Meter fix	1201	788	$y = 411x + 789^*$	D	1

Table 1: Altitude error standard deviation model segment's detailed values

*The x in the third equation is relative to the reference scale axis in Figure 9

model data (the regression analysis curve data points), respectively [16]. The regression curves with the highest correlation coefficients were then chosen to represent the model of the observed data. The choice between a linear or a quadratic function to represent the data was based on the correlation coefficients. The linear fit was chosen if its correlation was greater than or equal to 0.95; if not, the quadratic fit was chosen instead. In this way a high correlation between the observed data and the model was achieved.

9 Final Model

The final standard deviation model is presented in Table 1 and plotted with the data from Figure 6 and Figure 7 in Figure 8 and Figure 9. The dependent variable y in Table 1 is the altitude error standard deviation in feet; the independent variable x is altitude in feet for the first two equations and is relative to the reference scale in Figure 9 for the third equation. The high correlation values from the exhaustive search algorithm confirmed the use of three segments, as identified in the initial steps of the analysis.

The first model segment describes the initial error growth after the predicted TOD⁵; at the end of the segment the altitude error standard deviation reaches almost 2,500 feet. The second segment starts 8,000 feet below TOD, when the error standard deviation starts to decrease, and ends at the predicted BOD where the altitude error standard deviation is 1,366 feet. From BOD to the meter fix, the decay rate is faster reaching a final value of less than 800 feet (Figure 9). The prediction error rapidly decreases as the prediction approaches the meter fix since the aircraft's FMS is attempting to achieve the meter fix altitude constraint.

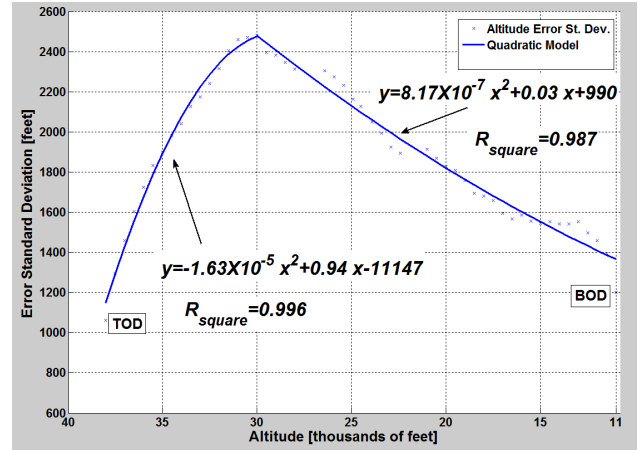


Figure 8: Altitude error standard deviation final model

With this model, the evolution of the altitude error standard deviation was completely characterized. For each segment, the model defines the initial and final values and an equation that describes the evolution (growth or decay) of the altitude error standard deviation (Table 1). The initial value of one segment doesn't have to be the same as the final value of the previous, as happens between segments two and three. These are just parameters that can be input independently in the CD algorithm [9].

In order to complete the quantification of the CTAS analytic probabilistic model, the evolution of the mean altitude error needed to be characterized and quantified along the CDA trajectory. This was necessary because from the data analyzed (e.g., Figure 3), the model assumption of zero mean error was clearly not valid.

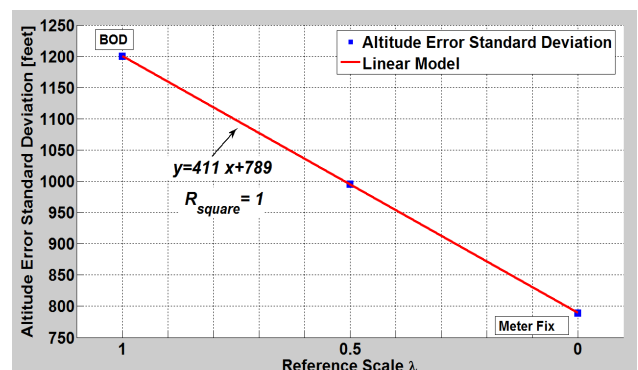


Figure 9: Altitude error standard deviation final model for the third segment

To properly validate this assumption of the model a larger sample of flights would have been needed. Nonetheless a framework on how

⁵ The altitude error before TOD, present only for the three Dallas flights is not captured in these plots.

the validation would have been approached will be briefly discussed. The aggregation of the flight sample over altitude steps provided the data points to calculate the statistics necessary for the validation of the basic model assumptions of zero mean and normal distribution of the altitude error.

Plotting the error distributions at each altitude step into histograms (Figure 10) shows how neither assumption is valid at least for the limited flight sample analyzed. For larger samples, a hypothetical normal distribution can be overlaid on the histogram to judge its quality of fit, or the data can be graphed on a normal probability plot (in which data would fall along a straight line if their actual distribution were normal) [17] in order to test the validity of the normal-distribution assumption.

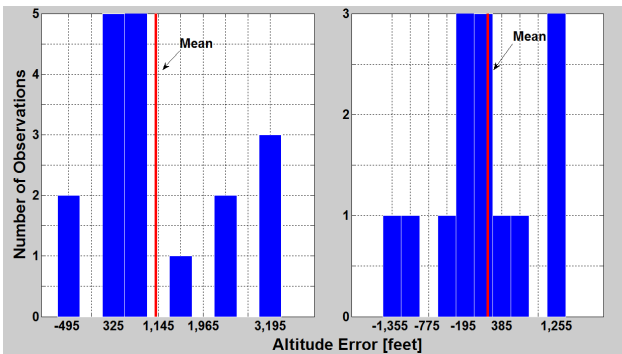


Figure 10: Altitude error histogram example

The model of the mean altitude error was then calculated using the same techniques as for the standard deviation model, producing the model in Figure 11 and Figure 12. The mean altitude error model consists of four segments (Table 2). Because most of the flights descended before the predicted TOD, the initial mean value is negative. Then, as can be generally seen in the plots from Figure 3, the mean altitude error grows rapidly, eventually reaching a maximum value of almost 1,900 feet (first segment in Figure 11). It then shrinks to a 1,090 feet (second segment), ramps up to 1,100 (segment 3) and then shrinks to the final value of less than 160 feet at the meter fix (Figure 12).

With the mean error model the characterization of the altitude error evolution over the sample of flights analyzed was complete. The CTAS uncertainty estimation model was completely defined for the data set. For each predicted altitude and along-path distance between TOD and meter fix, using the correlation approach explained in section 6, the expected error magnitude (mean) and scatter (standard deviation) can be calculated from the provided mathematical equations.

Segment	Altitude Range	Mean Initial Value (ft)	Mean Final Value (ft)	Evolution Equation (x = altitude in feet)*	Growth/Decay	Correlation coefficient with observed data
1	TOD→ TOD-4.5k	-460	1788	$y = -1.08 \times 10^{-4}x^2 + 7.23x - 119090$	G	0.999
2	TOD-4.5k→ BOD+1k	1768	1091	$y = -3.01 \times 10^{-6}x^2 + 0.17x - 497$	D	0.992
3	BOD+1k→ BOD	1100	1103	$y = -1.76 \times 10^{-5}x^2 + 0.40x - 1184$	G	1
4	BOD→Meter fix	1100	158	$y = 942x + 158 *$	D	0.999

Table 2: Mean altitude error model segment’s detailed values

*The x in the fourth equation is relative to the reference scale axis in Figure 12.

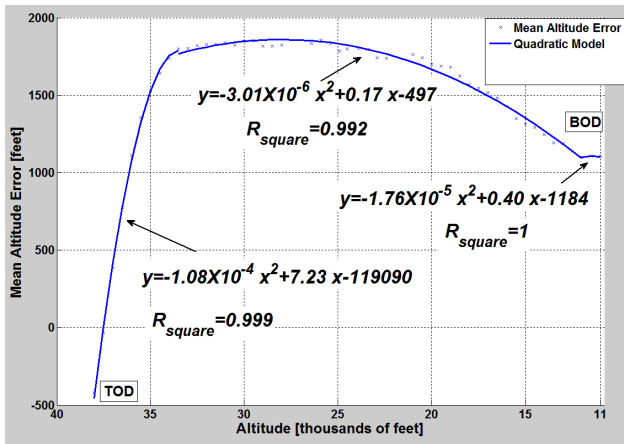


Figure 11: Mean altitude error final model

A plot of the final uncertainty model is presented in Figure 13. The mean and standard deviation values are plotted at each altitude step (converted to a predicted along path distance) and along-path distance event between the predicted TOD and meter fix on a representative (actual flight’s) predicted CDA trajectory. The mean value in the plot was added to the reference predicted trajectory along the CDA. The (spatially correlated) actual trajectory for this flight is also plotted.

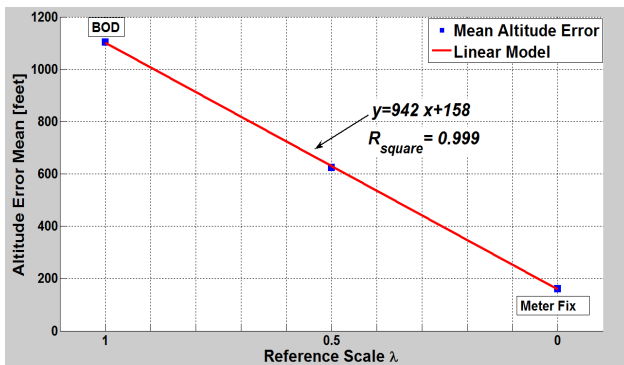


Figure 12: Mean altitude error final model for the fourth segment

The model of uncertainty was quantified as a function of the decreasing altitude from the TOD because the approach used to aggregate the flights in the sample was based on spatial correlation at significant points along the descent trajectory (TOD, BOD, and meter fix). There is a one-to-one correlation between the predicted altitude and the predicted time of any point in the predicted trajectory that can be used to directly convert the model from altitude-based/along-path distance-based to time-based.

Though straightforward, this would be required to implement the model in CTAS.

9 Discussion and Lesson Learned

A demonstration of using trajectory prediction accuracy techniques to define and quantify the parameters of a real-time uncertainty estimation model has been provided. By using actual prediction errors calculated from sampled flight data, the methodology enables capturing the cumulative effect of multiple prediction error sources, both known and unknown, within the resultant uncertainty model. Since the magnitude and evolution of prediction error typically varies along the nominal prediction, the methodology also accommodates the identification of an appropriate number of uncertainty model segments, each with its own parameters, as well as when to transition between these segments.

If proper flight sampling of the target environment is achieved, the quantified uncertainty model can be added to a TP to support the operations of its DST in the presence of prediction uncertainty. Although not intended to directly improve the TP itself, the addition of the uncertainty model, through the implementation of the system equations, can improve the overall performance of the DST.

The demonstrated application of the methodology to quantify the CTAS analytic probabilistic model for CDA operations illustrates one such DST application where proper handling of prediction uncertainty is likely to be a key enabling element. Another example is the sizing of the prediction uncertainty bounds of the Autonomous Operation Planner (AOP) [18], an airborne DST developed by NASA Langley Research Center to perform distributed separation assurance simulation experiments. The details of the AOP example are provided in reference [10]. Although demonstrated for specific uncertainty models, the methodology is general and can be used to instantiate a wide range of TP uncertainty models.

The CDA data used to quantify the CTAS analytic probabilistic model was sufficient to illustrate many of the strengths of the methodology, but it also pointed out some of the

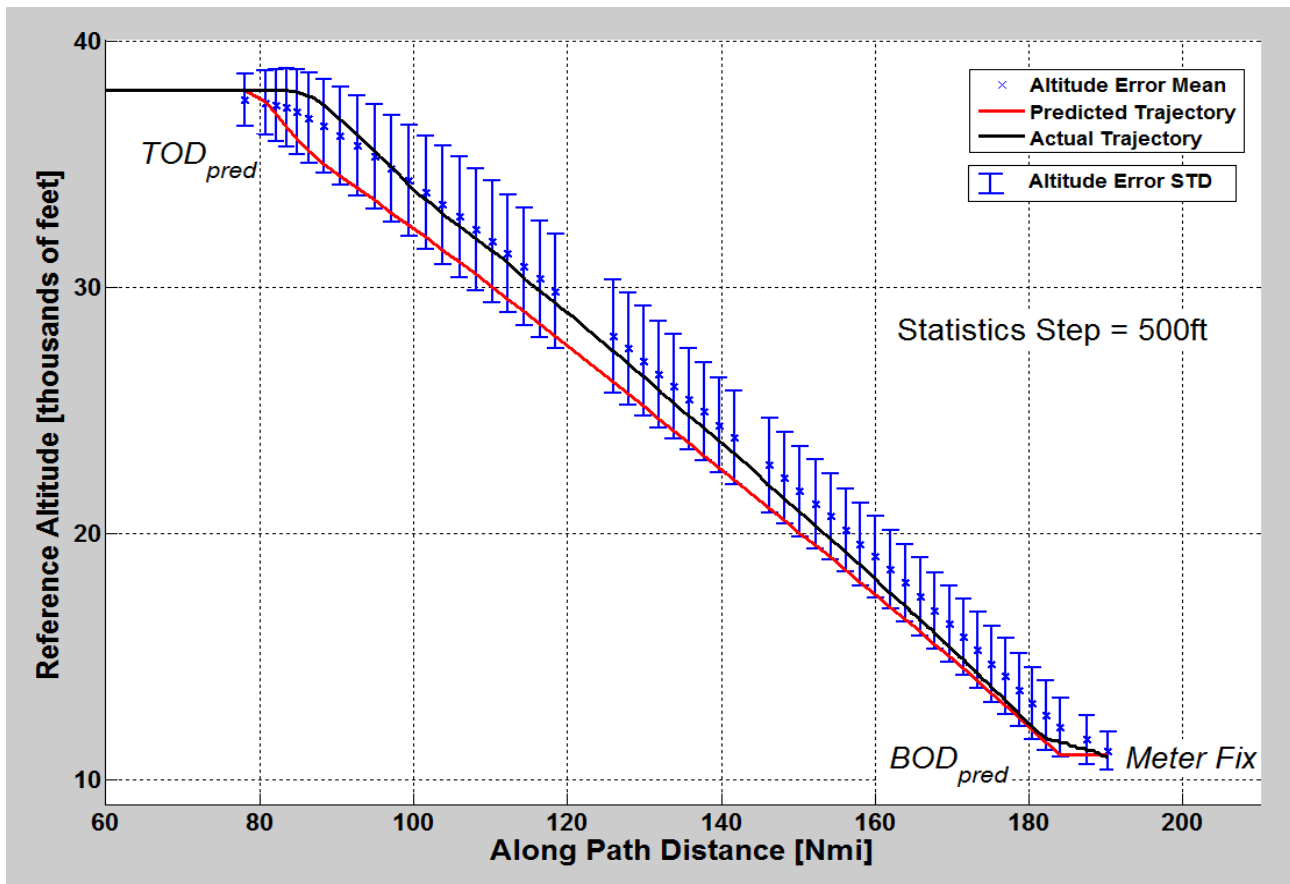


Figure 13: Uncertainty model final results visualization

issues that arise without a sufficient sample size. For example, due to the small sample size, it was not possible to validate that the prediction errors were normally distributed. Another example was the lack of enough data to properly handle the multiple descent altitude ranges. This issue influenced the choice to use a representative 27,000 feet CDA trajectory that makes the model very specific. These data limitations were caused by the necessity of using data collected from other CDA projects.

10 Conclusions and Future Work

The CTAS probabilistic uncertainty model for CDA operations was quantified using a methodology created previously. The assumptions of the model were also validated applying prediction accuracy analysis techniques to a small sample of flight collected from other research efforts on CDA operations.

The application of this methodology to a larger sample of flights would be a natural continuation of this work. Analyzing more

flights would give a wider scatter of descent trajectories with different descent lengths. The model therefore could be validated, with an independent sample, and generalized, or multiple models could be created if different aircraft would show significantly different behaviors.

Once a general model is obtained, how to implement the system equations calculated with the methodology into a DST could be an area of future research. Exploring how beneficial the uncertainty model could be on the DST operational performance.

Another possible extension of the work presented in this paper could be the quantification of the uncertainty model for the other two dimensions (cross- and along-track) of the TP error. Analyzing the along-track error would probably be more interesting than the cross-track, because the along-track error is strongly influenced by speed and wind errors that are usually significant sources of TP inaccuracy.

Acknowledgments

The authors would like to thank Jose Garcia-Chico for the preliminary research made to identify the uncertainty models present in the literature and Vincent Kuo for the discussions and the analysis of the AOP data set. The authors would also like to thank Huabin Tang, Steve Green, Todd Farley and Banavar Sridhar at NASA Ames Research Center for the valuable review that significantly improved this paper.

References

- [1] Joint Planning and Development Office, *Next Generation Air Transportation System Integrated Plan*, Version 2.0, 2007.
- [2] SESAR Consortium, *The ATM Target of Operations*, Technical Report No. DLT0612-001-02-00, Toulouse, France, 2007.
- [3] Green, S., Vivona, R., En Route Descent Advisor concept for arrival metering, *Proceedings of the AIAA Guidance, Navigation and Control Conference*, Montreal, Canada, AIAA-2001-4114, 2001.
- [4] Copenbarger, R., Mead, R., Sweet, D. Field evaluation of the tailored arrivals concept for datalink-enabled continuous descent approach, *Proceedings of the 7th AIAA Aviation Technology, Integration and Operations Conference*, Belfast, Northern Ireland, AIAA-2007-7778, 2007.
- [5] Green, S., Vivona, R., Sanford, B. Descent Advisor preliminary field test, *Proceedings of the AIAA Guidance, Navigation and Control Conference*, Baltimore, MD, AIAA-1995-3368, pp. 1777-1787 1995.
- [6] Green, S., Vivona, R. Field evaluation of Descent Advisor trajectory prediction accuracy, *Proceedings of the AIAA Guidance, Navigation and Control Conference*, San Diego, CA, AIAA-1996-3764, 1996.
- [7] Green, S., Vivona, R., Grace, M. Field evaluation of Descent Advisor trajectory prediction accuracy for en-route clearance advisories, *Proceedings of the AIAA Guidance, Navigation and Control Conference*, Boston, MA, AIAA-1998-4479, 1998.
- [8] Paielli, R., Erzberger, H. Conflict probability estimation for free flight, *Journal of Guidance, Control, and Dynamics*, Vol. 20, No 3, pp 588-596, 1997.
- [9] Paielli, R., Erzberger, H. Conflict probability estimation generalized to non-level flight, *Air Traffic Control Quarterly*, Vol. 7, No, 3, pp 195-222, 1999.
- [10] Enea, G., Karr, D. Kuo, V., Vivona, R., Applications and demonstration of a methodology for extending prediction accuracy analysis to uncertainty estimation, NASA Contract Report under revision for publication, Jan. 2010.
- [11] Paielli, R. Empirical test of conflict probability estimation, *Proceedings of the 2nd USA/Europe Air Traffic Management R&D Seminar*, Orlando, FL, 1998.
- [12] Civil Aviation Authority, *Noise from arriving aircraft: an industry code of practice*, Sep. 2001.
- [13] Roach, K., Analysis of American Airlines continuous descent approaches at Dallas/Fort Worth Airport, NASA NTX Internal Paper, 2008.
- [14] Sprong, K., Klein, K., Shiotsuki, C., Arrighi, J., Liu, S. Analysis of AIRE continuous descent arrival operations at Atlanta and Miami, *Proceedings of the 27th Digital Avionics System Conference*, Saint Paul, MN, pp. 3.A.5-1 - 3.A.5-13, 2008.
- [15] Ryan, H., Paglione, M., Green, S., Review of trajectory accuracy methodology and comparison of error measurement metrics, *Proceedings of the AIAA Guidance, Navigation, and Control Conference*, Providence, RI, AIAA-2004-4787, 2004.
- [16] Conover, W. *Practical nonparametric statistics*, 3rd Edition, John Wiley & Sons, New York, NY, 1999.
- [17] NIST/SEMATECH e-Handbook of statistical methods, <http://www.itl.nist.gov/div898/handbook/>, January 2009.
- [18] Karr, D., and Vivona, R. Conflict detection using variable four-dimensional uncertainty bounds to control missed alerts, *Proceedings of the AIAA Guidance, Navigation, and Control Conference*, Colorado, CO, AIAA-2006-6057, 2006.

Copyright Statement

The authors confirm that they, and/or their company or organization, hold copyright on all of the original material included in this paper. The authors also confirm that they have obtained permission, from the copyright holder of any third party material included in this paper, to publish it as part of their paper. The authors confirm that they give permission, or have obtained permission from the copyright holder of this paper, for the publication and distribution of this paper as part of the ICAS2010 proceedings or as individual off-prints from the proceedings.